Supplement

Title: High Temporal and Spatial Nitrate Variability on an Alaskan Hillslope Dominated by Alder Shrubs

Authors: R. E. McCaully[1,2], C.A. Arendt[1,2], B. D. Newman[1], V. G. Salmon[3], J. M. Heikoop[1], C. J. Wilson[1], S. A. Sevanto[1], N. A. Wales[1], G. B. Perkins[1], O. C. Marina, and S. D. Wullschleger[3]

Sample Collection

Soil pore water: Soil pore water samples were collected by installing macro-rhizons (Rhizosphere Research Products; hereby referred to as rhizons) using the methods described by Seeberg-Elverfeldt (2005). Rhizons, which have a porous tip through which water can pass free of ion exchange, were installed at depths between 15-30 cm, and due to the volume required for chemical analyses, were installed in nests (on average 5 rhizons per nest) at each sampling location depending on soil saturation and water availability. Soil pore water was collected in 60- ml syringes connected by luer-lock mechanisms on each rhizon. Syringes were subsequently combined into one sample per nest to obtain adequate volumes for analyses and ensure a homogenous bulk sample. Syringes were re-hung from rhizons at their respective sampling locations and left overnight before collection the next day.

In-field parameters: In-situ parameters were measured for each water sample and included depth to frozen soil or bedrock, soil temperature, soil pore water pH, dissolved oxygen, and specific conductivity. A 1 m steel frost probe was used to measure the depth (cm) to frozen soil, roots, or bedrock at each location. Depths were averaged from three measurements per rhizon nest. Soil temperature was measured in tandem with soil depth measurements using an Orion thermometer. An Orion pH meter and YSI multi-parameter meter were used to collect *in situ* hydrochemistry parameters in unfiltered samples upon collection. Dissolved oxygen (DO) was measured in July 2017 and 2018 using a Hach Portable Optical DO Probe or YSI multi-parameter meter.

Analysis

Soil pore water: Samples were immediately filtered with a 1.5 μm pre-filter and a 0.45 μm filter and stored in HDPE Nalgene bottles for major cation and anion analysis. Anion samples were frozen and cation samples were preserved to a pH < 2 with nitric acid and frozen. Cations were measured using inductively coupled plasma optical emission spectrometry (ICP-OES) on a Perkin Elmer Optima 2100DV instrument (Perkin Elmer Inc., USA) using United States Environmental Protection Agency (EPA) method 200.7; precision is justified to 0.01 mg L^{-}. Anions were measured with ion chromatography on a Dionex ICS-2100 instrument (Thermo Fisher Scientific Inc., USA) utilizing EPA method 300 (Throckmorton *et al*., 2015); precision is justified to 0.01 mg L^{-1}. Ammonium (NH_4^+) concentrations were determined for a subset of samples (n = 92) with a modified Berthelot method with a limit of quantitation of 0.03 mg L^{-1} by UV-VIS spectroscopy using a Cary 100 Bio UV-Visible Spectrophotometer (Agilent Inc., USA).

Isotopic data for $\delta^{15}N$ and $\delta^{18}O$ of NO_3^- were measured using the methods outlined in Heikoop *et al.,* (2015), where a modified denitrifier method outlined by Sigman *et al*., (2001) and Casciotti *et al*., (2002) using a GV Isoprime isotope ratio mass spectrometer (IRMS) coupled to a TraceGas peripheral instrument. Isotopic data for $\delta^{18}O$ - H_20 was measured using a GV Instruments Multiflow peripheral instrument coupled to a GV Isoprime IRMS (Heikoop *et al*., 2015). Isotope values of nitrate and water are reported in delta (δ) notation in parts per thousand (‰) as the deviation from a standard of known composition, atmospheric N_2 for NO_3^- and VSMOW (Vienna Standard Mean Ocean Water) for water.

Soil and leaf litter: Pebbles, roots, and leaf litter were removed from the tins upon collection to avoid any mass bias. Gravimetric soil moisture was measured where soil and tins were weighed, dried at 80° C for a minimum of 72 hours, and reweighed. Soil moisture was determined as the difference in mass between wet and dry soil. Thirteen soil samples and five leaf litter samples were analyzed for total N, $\delta^{15}N$ of soil organic nitrogen (SON) and C/N ratios using a Costech Elemental Analyzer coupled to a Thermo Delta V IRMS.

Coefficient of Variability

The coefficient of variability was calculated for Ca, Na, Cl^- and NO_3^- (Table S6) to directly compare the variability of each constituent across the landscape, where ratios closer to zero indicate less variation (Brown, 1998). Ca, Na, and Cl^- are all compounds that typically have low variability within the environment. Consistently high ratios of NO_3^- (> 1.5) and low ratios of Ca, Cl^-, and Na (< 1.5) indicate additional (biological) processes acting on NO_3^- production.

Supplemental Tables

Table S1: Ammonium concentrations measured in September 2017, July 2017, and September 2019. Values < 0.02 mg L^{-1} are not reported. Black horizontal lines separate sampling campaigns.

Date	*Chemical Parameter (mg L^{-1})*	*n*	*max*	*min*	*mean*	*std*
July-17	NH_4^+	1	0.08	0.08	-	-
Sept-17	NH_4^+	2	0.29	0.03	0.16	0.18
July-18	NH_4^+	13	0.08	0.02	0.04	0.02

Table S2: *In situ* chemical parameters measured during each sampling campaign. No measurements were collected in September 2018. Black horizontal lines separate sampling campaigns.

Date	***Chemical parameter***	***n***	***min***	***max***	***mean***	***std***
17-Jul	Dissolved Oxygen (mg L^{-1})	45	1.93	7.98	4.71	1.72
	pH	48	4.97	7.34	5.76	0.54
	Conductivity (μS cm^{-1})	-	-	-	-	-
17-Sep	Dissolved Oxygen (mg L^{-1})	3	3.86	7.04	4.97	1.79
	pH	20	4.74	6.42	5.47	0.44
	Conductivity (μS cm^{-1})	-	-	-	-	-
18-Jul	Dissolved Oxygen (mg L^{-1})	114	1.34	6.76	3.54	1.15
	pH	114	3.77	9.97	5.41	0.67
	Conductivity (μS cm^{-1})	114	0.02	0.16	0.07	0.04

Table S3: Coefficient of variability ratio for calcium, sodium, chloride, and nitrate on upland and lowland locations. July 2017 through September 2018. Black horizontal lines separate sampling campaigns.

Date	***Location***	***Ca***	***Na***	***Cl^-***	***NO_3^-***
All	Upland	0.69	0.43	1.40	1.89
	Lowland	0.88	0.27	1.24	2.08
Jul-17	Upland	0.41	0.29	1.22	2.02
	Lowland	0.77	0.35	1.18	1.17
	All Locations	0.90	0.34	1.35	3.29
Sep-17	Upland	0.46	0.14	0.55	1.45
	Lowland	0.38	0.14	0.67	2.11
	All Locations	0.46	0.33	0.93	2.03
Jul-18	Upland	0.51	0.27	0.43	1.06
	Lowland	0.71	0.20	0.30	1.97
	All Locations	0.901	0.28	0.40	1.56
Sep-18	Upland	0.85	0.48	1.01	1.39
	Lowland	0.89	0.22	0.25	1.97
	All Locations	1.02	0.49	1.09	2.35

Table S4: Soil depth (cm) and soil moisture (%) measured in July and September (2017) and July (2018). Location indicates the alder shrubland patches from which measurements were derived. 'UA', 'WA', and 'DA' denote locations upslope, within, and downslope of alder shrublands, respectively. Black horizontal lines separate sampling campaigns.

Date	***Parameter***	***Location***		***n***	***max***	***min***	***mean***	***std***
Jul-17	Depth (cm)	A1-A5	UA + WA	3	38.3	32.7	35.2	2.9
			DA	5	33	25.5	29.4	3.0
	Moisture (%)		UA + WA	19	67.7	4.3	28.5	23.8
			DA	8	83.9	8.9	55.9	20.9
Sep-17	Depth (cm)	A1/A4	UA + WA	9	66.0	43.6	45.7	21.7
			DA	5	66.7	48.8	56.5	5.4
	Moisture (%)		UA + WA	6	56.1	17.1	28.4	14.2
			DA	-	-	-	-	-
Jul-18	Depth (cm)	A1/A4	UA + WA	12	56	29.2	36.6	7.3
			DA	24	76.2	35.2	53.3	12.1
	Moisture (%)		UA + WA	7	57.6	16.2	36.7	14.9
			Downslope	18	82.7	19.2	51.0	22.6

Table S5: July 23-27, 2018 and September 21-22, 2018. Chemical parameters and constituents (Sample mean and standard deviation). Samples starting with P indicate Pits dug along the A1 transect. Concentrations without a reported standard deviation are single values.

July 23-27, 2018

Sample ID	*NO_3^- (mg L^-)*	*NO_3^- std*	*Mn (mg L^-)*	*Mn std*	*Fe^{2+} (mg L^-)*	*Fe^{+2}std*	*SO_4^{2-} (mg L^-)*	*SO_4^{2-} std*
A1_WI_Up	6.52	1.24	0.01	0.00	0.70	0.17	0.44	0.19
A1_WI_Mid	0.51	0.42	0.01	0.00	0.26	0.11	0.51	0.31
A1_WI_Down	0.82	0.98	0.01	0.00	0.22	0.06	0.27	0.12
A1_DS_Seep	0.65	0.11	0.00	0.00	<0.01	<0.01	1.27	0.04
A1_DS_0	4.57	0.35	0.02	0.02	0.47	0.02	0.33	0.13
A1_DS_10	0.02	0.01	0.00	0.00	0.58	<0.01	0.39	0.25
A1_DS_20	0.43	0.10	0.01	0.00	0.31	0.06	1.77	0.22
A1_DS_30	0.03	0.02	0.00	0.00	0.69	0.06	0.65	0.25
A1_DS_40	0.07	0.04	0.00	0.00	0.77	0.01	0.42	0.24
A1_DS_50	0.02	0.01	0.01	0.00	0.67	<0.01	0.39	0.26
A4_WI_Up	5.73	-	0.02	-	0.46	-	1.83	-
A4_WI_Mid	0.70	0.48	0.01	0.00	0.32	0.03	0.53	0.43
A4_WI_Down	2.50	0.45	0.01	0.00	0.2	0.17	0.59	0.49
A4_DS_0	2.08	0.96	0.00	0.00	0.03	0.02	4.50	0.40
A4_DS_10	0.04	0.06	0.03	0.02	0.73	0.90	0.66	0.20
A4_DS_20	0.03	0.04	0.05	0.01	5.21	3.05	0.52	0.23
A4_DS_30	0.02	0.02	0.32	0.05	1.99	1.96	0.62	0.23
A4_DS_40	0.03	0.03	0.12	0.02	1.00	1.05	1.11	0.61
A4_DS_50	0.03	0.03	0.06	0.09	1.87	-	0.55	0.15
Between A1/A4	0.15	0.09	0.01	0.01	0.36	0.09	0.78	0.35
P1_20	6.52	2.01	0.00	0.00	0.11	-	0.35	0.26
P1_40	7.59	2.03	0.01	0.00	0.53	-	0.31	0.09
P2_20	3.57	0.67	0.01	0.01	0.44	-	1.40	0.21
P2_40	8.01	0.25	0.00	0.00	0.22	-	1.83	0.27
P2_60	8.32	1.64	0.01	0.00	0.15	-	5.23	0.46
P3_20	0.03	0.01	0.00	0.00	0.64	-	0.54	0.22
P3_40	0.03	0.02	0.01	0.00	0.15	-	3.41	0.43

September 21-22, 2018

Sample ID	*NO_3^- (mg L^-)*	*NO_3^- std*	*Mn (mg L^-)*	*Mn std*	*Fe^{2+} (mg L^-)*	*Fe^{+2}std*	*SO_4^{2-} (mg L^-)*	*SO_4^{2-}std*
A1_WI_Up	17.73		0.01		0.57		0.22	
A1_WI_Mid	0.58	0.70	0.01	0.02	0.15	0.05	0.20	0.07
A1_WI_Down	1.45	0.75	0.01	0.00	0.18	0.10	0.15	0.04
A1_DS_Seep	0.74	0.24	0.00	0.00	0.00	0.00	35.51	10.52
A1_DS_0	3.11	0.81	0.00	0.00	0.68	0.13	0.20	0.01

A1_DS_10	0.06	0.06	0.00	0.00	0.60	0.06	0.23	0.10
A1_DS_20	0.10	0.01	0.00	0.00	0.26	0.20	1.71	0.46
A1_DS_30	0.02	0.01	0.00	0.00	0.90	0.28	0.41	0.08
A1_DS_40	0.03	0.01	0.00	0.00	0.64	0.08	0.28	0.10
A1_DS_50	0.02	0.01	0.00	0.00	1.72	0.83	0.19	0.06
A4_WI_Mid	3.21	2.78	0.04		0.11	0.02	0.23	0.04
A4_WI_Down	8.44	3.44	0.01	0.01	0.10	0.03	0.29	0.16
A4_DS_0	3.44	2.70	0.00	0.00	0.05	0.01	5.01	0.33
A4_DS_10	0.05	0.05	0.02	0.01	1.33	0.74	5.65	6.12
A4_DS_20	0.02	0.01	0.04	0.01	4.60	1.39	1.60	1.53
A4_DS_30	0.02	0.00	0.22	0.12	1.92	1.15	0.56	0.41
A4_DS_40	0.04	0.04	0.11	0.03	6.75	4.74	1.56	0.49
A4_DS_50	0.03	0.03	0.23	0.23	13.31	7.19	0.25	0.04
Between A1/A4	0.38	0.08	0.00	0.00	0.21	0.21	0.93	0.39
P1_20	4.87	1.15	0.01	0.00	0.78	0.02	0.82	0.07
P1_40	5.45	0.06	0.00	0.00	0.18	0.03	1.56	0.02
P1_60	0.10	0.07	0.16	0.04	0.16	0.04	2.76	1.04
P2_20	0.04	0.00	0.00	0.00	1.34	0.60	0.53	0.23
P2_40	0.06	0.04	0.02	0.01	3.77	3.29	0.25	0.03
P3_20	29.22	10.74	0.00	0.00	0.29	0.03	0.23	0.03
P3_40	28.03	1.15	0.00		0.08		0.15	

Table S6: A statistical comparison of soil pore water concentrations (nitrate, ferrous iron, total iron, manganese, and sulfate, respectively) in upland locations compared to lowland locations along the A1 and A4 transects in 2018 (July and September campaigns combined). P-values < 0.05 are considered significant and indicate that 'upland' concentrations are significantly different from 'lowland' concentrations.

Chemical Parameter	*Transect*	*p - value*	*Upland (n)*	*Lowland (n)*
NO_3^-	A1	**<0.001**	31	58
	A4	**<0.001**	19	36
	Both	**<0.001**	56***	94
Fe^{2+}	A1	0.194	10*	15
	A4	**0.021**	6*	9*
	Both	**<0.004**	18***	24
Fe_{Total}	A1	**0.02**	31	58
	A4	**<0.001**	19	36
	Both	**<0.001**	56***	94
Mn	A1	<0.001**	31	58
	A4	**<0.001**	19	36
	Both	0.165	40***	94
SO_4^{2-}	A1	<0.001**	31	58
	A4	0.772	19	36
	Both	**<0.001**	56***	94

*Low *n* due to limited sampling equipment may result in unreliable p values.
**although significantly different, the average Upland Mn and SO_4^{2-} concentrations are greater than the average Lowland Mn concentration and thus do not indicate oxidizing conditions in the Upland area transitioning to reducing conditions in the Lowland area.
***'Upland' includes soil pore water collected both within and outside (between) alder shrublands.

Table S7: Oxygen isotopic composition from soil pore water. July 2017 through September 2018. Black horizontal lines separate sampling campaigns. P-values indicate significant difference between individual seasons and the total mean (All Seasons). P-values less than 0.05 are significant.

Date	*Isotope (‰)*	*n*	*min*	*max*	*mean*	*std*	*P-value*
17-Jul	$\delta^{18}O$	48	-17.3	-15.6	-16.5	0.4	0.42
17-Sep	$\delta^{18}O$	28	-17.0	-13.6	-15.6	0.8	**<0.001**
18-Jul	$\delta^{18}O$	116	-19.4	-14.4	-16.7	0.9	0.01
18-Sep	$\delta^{18}O$	80	-18.4	-12.3	-16.2	1.0	0.15
All Seasons	$\delta^{18}O$	272	-19.4	-12.3	-16.4	0.9	-

Supplemental Figures

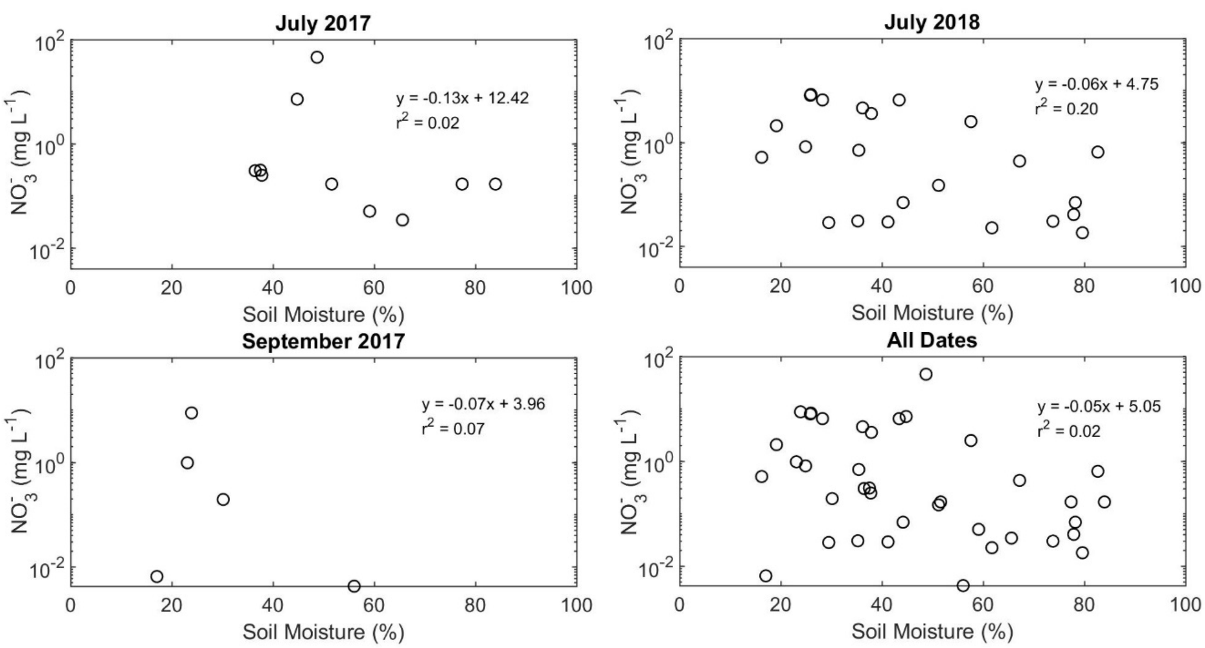

Figure S1: Soil moisture versus NO_3^- from July 2017, July 2018, September 2018, and all three seasons. No direct relationship was observed between soil pore water NO_3^- and soil moisture content.

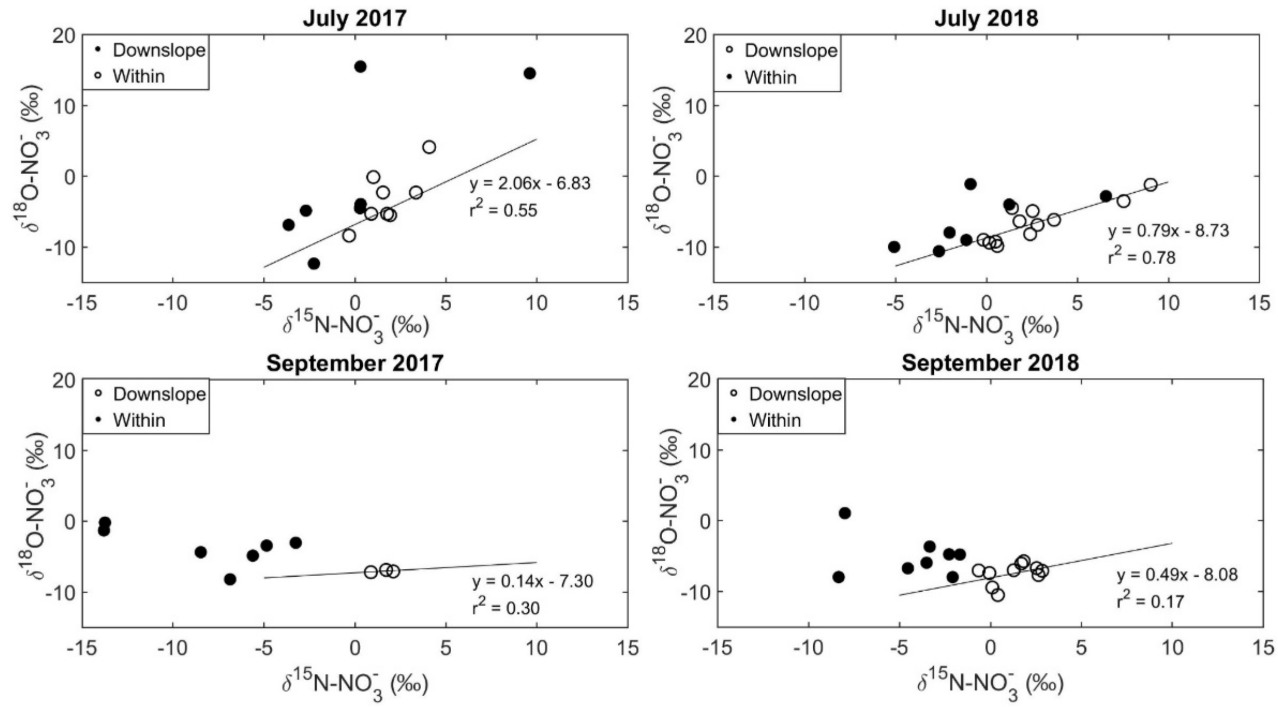

Figure S2: Oxygen ($\delta^{18}O$) versus nitrogen ($\delta^{15}N$) isotopes of soil pore water NO_3^- during July and September (2017 and 2018). Closed black circles represent samples from locations within alder shrubland patches and open black circles represent locations downslope of alder shrubland patches. Black trend lines and equations indicate enrichment of $\delta^{18}O$ and $\delta^{15}N$ of NO_3^- (indicating denitrification) occurring downslope of alder shrublands during each season.

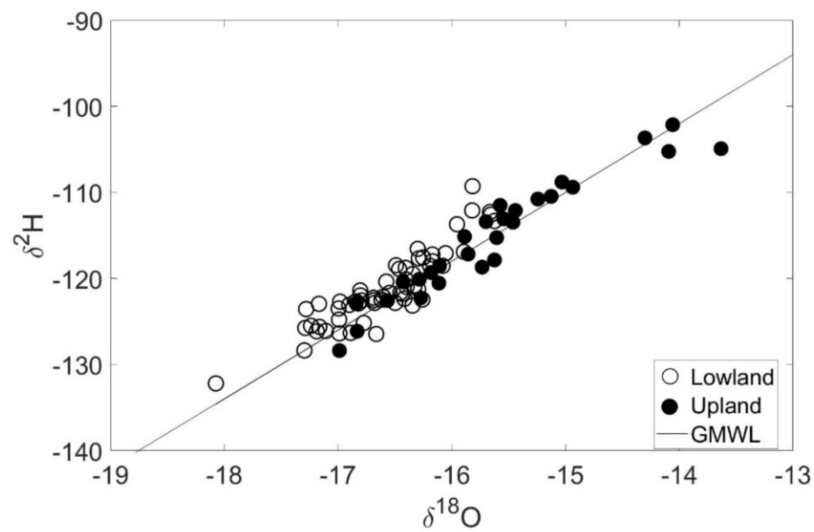

Figure S3: Soil pore water oxygen ($\delta^{18}O$) versus deuterium (δ^2H) isotopes during July 2017 and September of 2017 and 2018. $\delta^{18}O$ and δ^2H are plotted against the global meteoric water line (GMWL). Open circles represent lowland locations ($r^2 = 0.81$) and closed circles represent upland locations ($r^2 = 92$).

Supplemental References

Brown, C. E.: Coefficient of Variation, in: Applied multivariate statistics in geohydrology and related sciences, edited by: Brown, C. E., Springer, Berlin, Heidelberg, Germany, 155–157, https://doi.org/10.1007/978-3-642-80328-4_13, 1998.

Casciotti, K. L., Sigman, D. M., Hastings, M. G., Böhlke, J. K., and Hilkert, A.: Measurement of the oxygen isotopic composition of nitrate in seawater and freshwater using the denitrifier method, Analytical Chemistry, 74, 4905–4912, https://doi.org/10.1021/ac020113w, 2002.

Heikoop, J. M., Throckmorton, H. M., Newman, B. D., Perkins, G. B., Iversen, C. M., Chowdhury, T. R., Romanovsky, V., Graham, D. E., Norby, R. J., Wilson, C. J., and Wullschleger, S. D.: Isotopic identification of soil and permafrost nitrate sources in an Arctic tundra ecosystem, J. Geophys. Res. Biogeosci., 120, 1000– 1017, https://doi:10.1002/2014JG002883, 2015.

Sigman, D. M., Casciotti, K. L., Andreani, M., Barford, C., Galanter, M., and Böhlke, J. K.: A bacterial method for the nitrogen isotopic analysis of nitrate in seawater and freshwater, Analytical Chemistry, 73*,* 4145–4153, https://doi.org/10.1021/ac010088e, 2001.

Throckmorton, H. M., Heikoop, J. M., Newman, B. D., Altmann, G. L., Conrad, M. S., Muss, J. D., Perkins, G. B., Smith, L. J., Torn, M. S., Wullschleger, S. D., and Wilson, C. J.: Pathways and transformations of dissolved methane and dissolved inorganic carbon in Arctic tundra watersheds: Evidence from analysis of stable isotopes, Global Biogeochem. Cycles, 29, 1893–1910, https://doi:10.1002/2014GB005044, 2015.